Wave localization in number-theoretic landscapes

L. Dal Negro,[1,2,3,*] Y. Zhu,[3] Y. Chen ,[1] M. Prado ,[4] and F. A. Pinheiro [4]

[1]*Department of Electrical and Computer Engineering & Photonics Center,*
Boston University, 8 Saint Mary's Street, Boston, Massachusetts 02215, USA
[2]*Department of Physics, Boston University, 590 Commonwealth Avenue, Boston, Massachusetts 02215, USA*
[3]*Division of Material Science and Engineering, Boston University, 15 Saint Mary's Street, Brookline, Massachusetts 02446, USA*
[4]*Instituto de Física, Universidade Federal do Rio de Janeiro, Rio de Janeiro-RJ, 21941-972, Brazil*

We investigate the localization of waves in aperiodic structures that manifest the characteristic multiscale complexity of arithmetic functions with a central role in number theory. In particular, we study the eigenspectra and wave localization properties of tight-binding Schrödinger equation models with onsite potentials distributed according to the Liouville function $\lambda(n)$, the Möbius function $\mu(n)$, and the Legendre sequence of quadratic residues modulo a prime. We employ multifractal detrended fluctuation analysis and establish the multifractal scaling properties of the energy spectra in these systems. Moreover, by systematically analyzing the spatial eigenmodes and their level spacing distributions, we show the absence of level repulsion with broadband localization across the entire energy spectra. Our study introduces finite-size aperiodic systems whose eigenmodes are all strongly localized and provide opportunities for unique quantum and classical devices of particular importance to cold-atom experiments with engineered speckle potentials as well as unique optical metamaterials and nanostructures with enhanced light-matter interactions.

I. INTRODUCTION

The study of localized quantum and classical waves in randomly fluctuating potentials attracted intense research activities that unveiled deep analogies between the mesoscopic physics of electrons and photons with applications to advanced electronic and optical technologies [1–4]. In particular, starting from the pioneering paper of Anderson [5] and the discovery of quasicrystals [6], many important results have been obtained on the localization and wave diffusion properties of discrete systems with disordered as well as aperiodically ordered potentials [7–11]. Specifically, discrete systems with deterministic aperiodic potentials display very rich physical properties that are absent in both periodic (crystalline) and random (amorphous) states of matter. For example, their energy spectra are generally singular continuous and support eigenmodes characterized by highly fragmented, multifractal envelopes with various degrees of spatial localization, known as critical modes [12–15]. These enable control of anomalous wave transport phenomena that are somewhat intermediate between diffusive and ballistic ones [14,16–20]. Moreover, topologically protected edge states have been discovered recently in quasiperiodic chains, significantly broadening our understanding of topological phases beyond crystalline structures [21,22].

A considerable body of work is concerned with discrete one-dimensional (1D) structures consisting of linear chains with potentials generated by various deterministic aperiodic sequences [3,4,8,11,23–26]. Aperiodic order in potential scattering problems provides deterministic control over the rich physics of complex systems that are suitable for engineering device implementations within the available layer deposition and nanofabrication technology [27,28]. The prototypical model to describe transport of quantum and classical waves in these systems is based on the discrete Schrödinger equation in the tight-binding approximation

$$(\mathcal{H}\psi)_n = t\psi_{n-1} + t\psi_{n+1} + V_n\psi_n = E\psi_n, \qquad (1)$$

where ψ_n denotes the wave function at the nth site, t is a constant hopping rate, V_n are the values of onsite potential following an aperiodic sequence, and $\mathcal{H}$ defines the linear Schrödinger operator. It has been established that for a white-noise potential with correlation $\langle V_n V_m \rangle = \sigma^2 \delta_{nm}$, all the eigenstates of the tight-binding model are exponentially localized independently of the variance σ^2 of the disorder [9,29,30]. As a result, it is generally believed that in 1D random potentials the density of states becomes singular and all eigenstates are localized, leading to Anderson localization. However, not all states in 1D disordered systems are exponentially localized. Indeed, this traditional belief has been challenged by the discovery of fully extended states in disordered 1D systems, known as Azbel resonances, randomly distributed in the energy spectrum over a set of zero measure (and therefore generally neglected) [31,32].

Another delocalization mechanism in 1D disordered systems was predicted by Pendry [33], where nonlocalized modes exist that extend over the sample via multiple resonances, forming the so-called necklace states. These modes have transmission coefficient close to 1 and, although extremely rare, they can dominate the average transmission, as it has been observed in optical random systems [34,35]. Moreover,

*dalnegro@bu.edu

extended states have also been demonstrated in tight-binding disordered potentials with short-range correlations, called random dimer models, where are known to appear for any realization of the random potential [36–38]. In contrast, it was proven rigorously that 1D binary chains with Fibonacci, Thue-Morse, and period-doubling deterministic aperiodic potentials feature singular continuous spectra supported by a Cantor set with zero Lebesgue measure [39–41]. This general feature produces an infinity of pseudogaps with zero total bandwidth. In these structures, the locations and widths of the spectral gaps are determined by the local peaks of their Fourier spectra (i.e., their Fourier transforms) as precisely stated by the so-called "gap-labeling theorem" [42,43]. Moreover, the corresponding eigenstates are neither extended nor exponentially localized but exhibit intricate envelopes with power-law decay and fluctuations at multiple scales described by multifractal analysis, similarly to the geometry of strange attractors in complex dynamical systems [12,44–47]. In 1980, Aubry and André realized that certain quasiperiodic potentials that depend on a parameter can give rise to a localization phase transition that occurs in one dimension [48], which has been observed in noninteracting Bose-Einstein condensates [49]. This phenomenon is related to the rich behavior of the Harper's equation that describes electrons on two-dimensional lattices under perpendicular magnetic fields [50]. More recently, the interest on the Aubry-André model and its extensions have attracted much attention due to their applications to many-body localization [51,52]. Quasiperiodic potentials, such as the one of the kicked rotor model [53], are also known to induce wave localization in momentum space, which characterizes the phenomenon of dynamical localization observed in atom-optics systems [54].

Interestingly, extended states have also been discovered in Rudin-Shapiro aperiodic potentials that are fully deterministic but possess an absolutely continuous correlation measure (i.e., Fourier spectral measure) similarly to uncorrelated random sequences [55,56]. Furthermore, the absence of the localization regime has been recently shown in Rudin-Shapiro 1D potentials within the tight-binding model [57,58]. However, it is currently unknown if deterministic 1D aperiodic potentials exist that only support localized modes in their spectra. This not only poses an open conceptual question on the connection between the structural and localization properties of aperiodic systems, but also creates the opportunity to introduce novel structurally complex, yet deterministic structures, that achieve localization over their entire spectra in realistic finite-size implementations without the involvement of any statistical randomness. In order to address this fundamental problem, we recently introduced an approach that leverages the multiscale structural complexity inherent to number theory to achieve stronger wave localization and anomalous transport in resonantly scattering systems [4,59–64].

In this paper we focus on 1D tight-binding structures that enable the efficient exploration of large-scale aperiodic discrete systems with onsite potentials arranged according to important arithmetic functions of number theory. In particular, we consider the Liouville function $\lambda(n)$, the Möbius function $\mu(n)$, and the Legendre sequence of quadratic residues modulo a prime (QRs). We establish the multifractal nature of the tight-binding spectra using multifractal detrended fluctuation analysis (MDFA) and we systematically analyze the spatial distributions of eigenmodes through the mode spatial extent (MSE) analysis. Our findings reveal that all the eigenstates of the investigated systems are strongly localized, in contrast to 1D disordered systems, where delocalized modes can exist. These results are corroborated by the statistical analysis of the level spacing distribution, which shows the absence of the level repulsion. Thanks to the fundamental equivalence (i.e., isomorphism) between the Schrödinger and Helmholtz equations in the frequency domain, the introduced potential models provide opportunities for the engineering of quantum as well as optical metamaterials and photonic devices with broadband spectra of localized excitations, enabling tailored wave transport phenomena.

Our paper is organized as follows. In Sec. II we introduce the background on the considered arithmetic functions. The multifractality of their spectral density is discussed in Sec. III. Localization and level statistics are treated in Sec. IV and conclusions in Sec. V. Finally, in Appendixes A and B we discuss the results for the Legendre sequence and the structural correlation properties of the investigated arithmetic sequences, respectively.

II. ARITHMETIC FUNCTIONS BACKGROUND

The aperiodic structures considered in this paper are constructed based on important arithmetic functions in number theory. An arithmetic function $f(n)$ is any function whose domain is the set of positive integers and whose range is a subset of the complex numbers. Interesting arithmetic functions in number theory are the ones that encode nontrivial arithmetical properties of n. These generally display an extremely erratic and aperiodic behavior, which makes them an attractive tool for the implementation of very irregular deterministic scattering potentials. Specifically, in this paper we focus on the Liouville function $\lambda(n)$, the Möbius function $\mu(n)$, and the Legendre sequence generated from the distribution of quadratic residues modulo a prime (QRs) [65,66].

The Liouville function $\lambda(n)$ has a value equal to $+1$ if n is the product of an even number of prime numbers, and equal to -1 if it is the product of an odd number of primes. It can be defined by the simple formula $\lambda(n) = (-1)^{\Omega(n)}$, where $\Omega(n)$ is the prime omega function that counts the total number of prime factors of n, including their multiplicity. Interestingly, the Dirichlet series for the Liouville function is related to the Riemann zeta function as follows [67,68]:

$$\frac{\zeta(2s)}{\zeta(s)} = \sum_{n=1}^{\infty} \frac{\lambda(n)}{n^s}, \tag{2}$$

where $s \in \mathbb{C}$ with $\mathrm{Re}(s) > 1$. A plot of the first 200 values of $\lambda(n)$ is shown in the top panel of Fig. 1. The Liouville function manifests a complex aperiodic behavior with oscillations similar to an uncorrelated binary random function with no discernible patterns. Several fundamental results of number theory can be deduced assuming the uncorrelated randomness of $\lambda(n)$, most importantly, the prime number theorem (PNT) that follows from [67]:

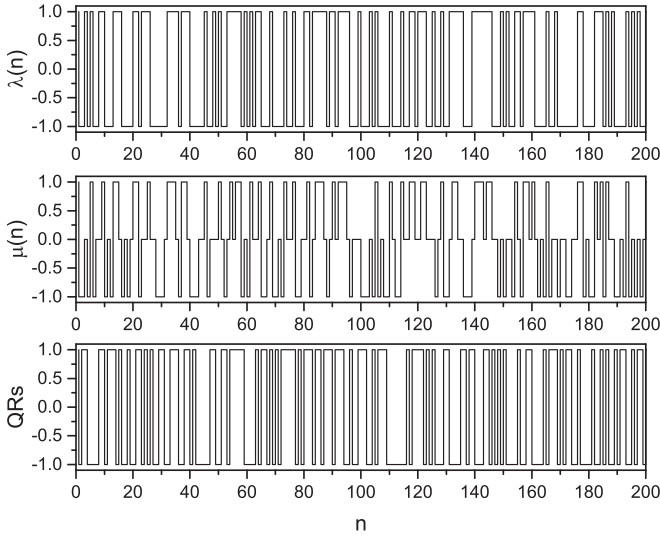$$\lim_{n \to \infty} \frac{\lambda(1) + \lambda(2) + \cdots + \lambda(n)}{n} = 0. \tag{3}$$

FIG. 1. The first 200 values of the Liouville $\lambda(n)$ function, Möbius function $\mu(n)$, and the distribution of quadratic resides QRs (Legendre sequence), respectively.

Moreover, the asymptotic behavior of the following sum of the Liouville function provides an equivalent formulation of the Riemann's hypothesis (RH):

$$\left| \sum_{n \leqslant N} \lambda(n) \right| \leqslant C_\epsilon N^{\frac{1}{2}+\epsilon}, \tag{4}$$

where C_ϵ and ϵ are positive constants [67]. The statement above implies that the values of $\lambda(n)$ behave similarly to a random sequence of 1's and -1's in that the difference between the number of 1's and -1's is not much larger than the square root of the number of terms [67,68].

The Möbius function $\mu(n)$ has values on the set $\{-1, 0, +1\}$ depending on the factorization of n into prime factors. In particular, $\mu(n) = +1$ if n is a square-free (i.e., an integer which is divisible by no square number other than unity) positive integer with an even number of prime factors, $\mu(n) = -1$ if n is a square-free positive integer with an odd number of prime factors, and $\mu(n) = 0$ if n has a squared prime factor. The first 200 values of the function $\mu(n)$ are plotted in the middle panel of Fig. 1. This function plays a central role in elementary and analytic number theory particularly in relation to the Dirichlet convolution and the Möbius inversion formula that connects two arithmetic functions. The Möbius function is also fundamentally related to the Liouville function in many ways [e.g., $\lambda(n)\mu(n) = \mu^2(n)$] and its Dirichlet series expression equals the inverse of the Riemann zeta function [65,68].

The last structure that we analyzed is the Legendre sequence constructed from the distribution of the quadratic residues modulo a prime p. An integer number n is a quadratic residue modulo p (mod p) if it is congruent to a perfect square, i.e., if there exists an integer number m such that $m^2 \equiv n \bmod p$. Otherwise, n is called a quadratic nonresidue mod p. The quadratic residues can simply be found by considering all numbers from 0 to $(p-1)/2$, squaring them, and taking the result mod p. By convention 0 is not con-

sidered a quadratic residue while 1 is a residue for every p. The quadratic residues form a multiplicative group and the nonresidues are the coset of that group. The first systematic theory of quadratic residues was developed by Gauss in his *Disquisitiones Arithmeticae* published in 1801, but important results and conjectures were already established by Fermat, Euler, Lagrange, Legendre, and other number theorists of the 17th and 18th centuries [65,69]. The Legendre sequence, whose first 200 values are plotted in the bottom panel of Fig. 1, has an absolutely continuous correlation measure that is akin to random sequences, and this fact has been exploited in applications to acoustics diffusers and cryptographic systems [70–72]. However, the quadratic residues modulo a prime also obey fundamental symmetries constrained by the quadratic reciprocity law and other remarkable regularities [65,69]. For an odd prime p and any rational integer q that is not a multiple of p it is customary to introduce the Legendre symbol $(\frac{q}{p})$ that equals $+1$ if q is a quadratic residue, -1 if q is a quadratic nonresidue modulo p, and it vanishes if q is a multiple of p. The binary Legendre sequence of length p (then repeating periodically) is defined as $L_q = (\frac{q}{p})$. This sequence encodes interesting eigenvectors of the Fourier transform operator and has many fascinating properties [73]. These include a flat power spectrum and a two-valued autocorrelation function with a peak at the origin and a constant value otherwise, with applications to coding, communications, and imaging devices based on coded apertures [72–74].

III. SPECTRAL MULTIFRACTALITY

In this section we study the energy spectra of the Liouville and the Möbius structures. The corresponding analysis for the Legendre sequence is provided in Appendix A. We consider the tight-binding Hamiltonian in Eq. (1) with hopping rate $t = 1$ (i.e., the energy is given in units of t). We enforce the zero boundary condition $\psi_0 = \psi_N = 0$ and obtain all the energy eigenvalues by direct diagonalization for systems with 3×10^4 sites (for the Legendre sequence we chose the prime $p = 29\,989$). In particular, we study the behavior of the integrated density of states (IDOS) defined as $\rho(\omega) = \int_0^\omega g(\omega')d\omega'$, which we show as a function of energy in Figs. 2(a) and 3(a) for the investigated structures. The obtained IDOS spectra are monotonically increasing functions featuring a staircase structure with very narrow plateaus and sharp jumps that can occur at all energy scales. We highlighted this characteristic spectral behavior by magnifying the IDOS curves inside two representative small regions of interest, indicated by the arrows drawn in Figs. 2(a) and 3(a). We conjecture that this characteristic steplike behavior of the spectral density of the Liouville and Möbius systems is a reflection of yet-undiscovered long-range structural correlations that are present in their aperiodic potential distributions. The energy spectra of aperiodic structures with singular continuous components possess distinctive fractal scaling properties that give rise to anomalous sub-diffusion phenomena as well as stronger localization effects [46,75]. Therefore, it is important to accurately investigate and characterize the spectral scaling properties of in the proposed structures.
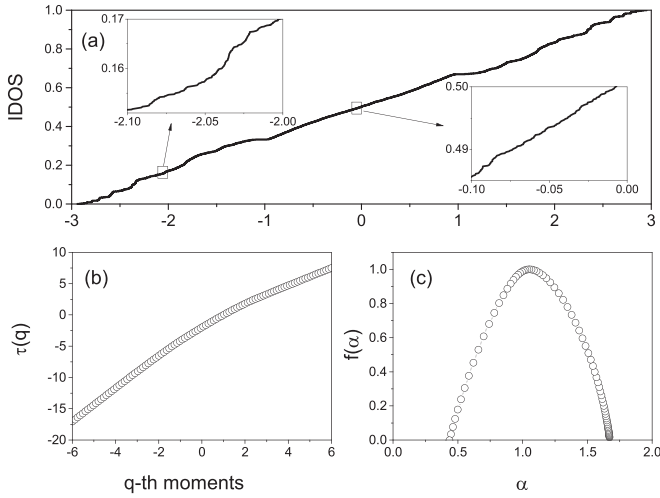
FIG. 2. (a) Integrated density of states (IDOS) for the Liouville structure. The insets show magnified views of the IDOS within the small rectangular regions of interest identified. (b) Mass exponent (scaling function) $\tau(q)$ and (c) multifractal spectrum $f(\alpha)$ of the spectrum shown in (a).

In order to characterize these properties, we apply the multifractal detrended fluctuation analysis (MDFA) [76] using the numerical routines developed by Ihlen for the study of nonstationary multiscale signals [77]. The MDFA is a powerful technique that extends the traditional detrended fluctuation analysis (DFA) [78] to the case of nonstationary time series with multifractal scaling properties. The MDFA enables accurate determination of the multifractal parameters of a signal, including its multifractal spectrum [76]. This is achieved by considering the local scaling of fluctuations with respect to smooth trends over piecewise sequences of locally approximating polynomial fits, i.e., $F_q(n) \propto n^{h(q)}$ where $h(q)$ is the generalized Hurst exponent, or q-order singularity expo-
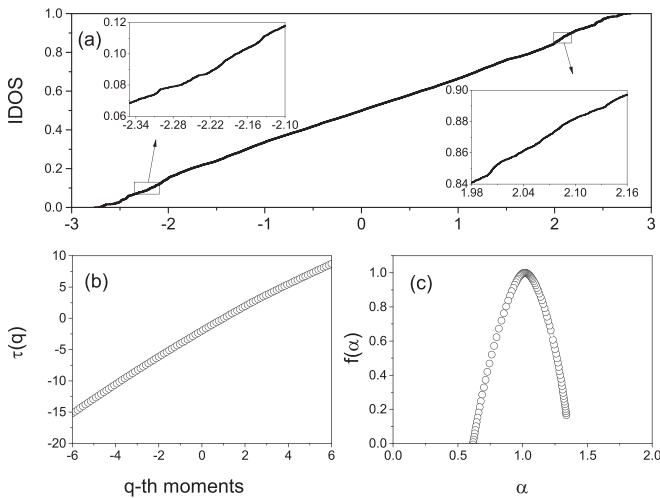

FIG. 3. (a) Integrated density of states (IDOS) for the Möbius structure. The insets show magnified views of the IDOS within the small rectangular regions of interest identified. (b) Mass exponent (scaling function) $\tau(q)$ and (c) multifractal spectrum $f(\alpha)$ of the spectrum shown in (a).

nent [77]. The generalized parameter $h(q)$ reduces to the Hurst exponent $H \in [0, 1]$ for stationary signals [76,77]. In our analysis the multifractal IDOS signal x_t is regarded as a discrete series of data points labeled by the integer parameter t and the generalized fluctuations $F_q(n)$ are defined as the q-order moments over N intervals of size n according to [61,76,77]

$$F_q(n) = \left(\frac{1}{N} \sum_{t=1}^{N} (X_t - Y_t)^q \right)^{1/q}, \qquad (5)$$

where

$$X_t = \sum_{k=1}^{t} (x_k - \langle x \rangle). \qquad (6)$$

Here Y_t denotes the piecewise sequence of approximating polynomial trends obtained by local least-squares fits over sample segments of size n and $\langle x \rangle$ is the mean value of the analyzed time series corresponding to the IDOS signal. Finally, the multifractal spectrum $f(\alpha)$ of the spectrum is computed from the mass exponent $\tau(q)$ using the Legendre transform

$$D(\alpha) = q\alpha - \tau(q), \qquad (7)$$

where $\tau(q) = qh(q) - 1$ and $\alpha = \tau'(q)$ [76]. We show in Figs. 2(b) and 3(b) the computed mass scaling exponent $\tau(q)$ of the IDOS of the Liouville and Möbius structure, respectively. The nonlinear behavior of $\tau(q)$ reported in Figs. 2(b) and 3(b) is a characteristic signature of multifractality in the analyzed signals [61,76,77,79]. In Figs. 2(c) and 3(c) we display the corresponding multifractal spectra, which show single humped continuous functions with broad and downward concavities indicative of strong multifractality in the investigated systems. We recall here that the width $\Delta f(\alpha)$ of the support of a multifractal spectrum is a direct measure of its degree of nonhomogeneity [79]. Therefore, our results demonstrate that the Liouville and Legendre structures (see Appendix A) have similar multifractal spectra and their inherent structural complexity is significantly more inhomogeneous compared to the one of the Möbius structure, which in fact displays the narrowest multifractal spectrum.

IV. LOCALIZATION AND LEVEL STATISTICS

An important problem in the study of discrete structures with deterministic aperiodic potentials is related to understanding the nature of their eigenmodes. Aperiodic structures with multifractal energy spectra generally give rise to anomalous dynamic transport [46,83] but do not necessarily support eigenmodes with multifractal spatial properties. Generally, it is believed that quasiperiodic and fractal systems with singular continuous energy spectra, which often exhibit fractality in either physical or energy space, support critical eigenmodes that decay in real space weaker than exponentially, typically by following a power law. These modes feature a hierarchical structure of self-similar fluctuations that have been fully characterized using multifractal analysis in real space [45–47]. However, critical states originate from the resonant tunneling across similar subunits that repeat over different length scales, thus spatially extending over the entire structure [8,10,44].

To the best of our knowledge, it remains to be established if 1D finite-sized aperiodic structures can be deterministically
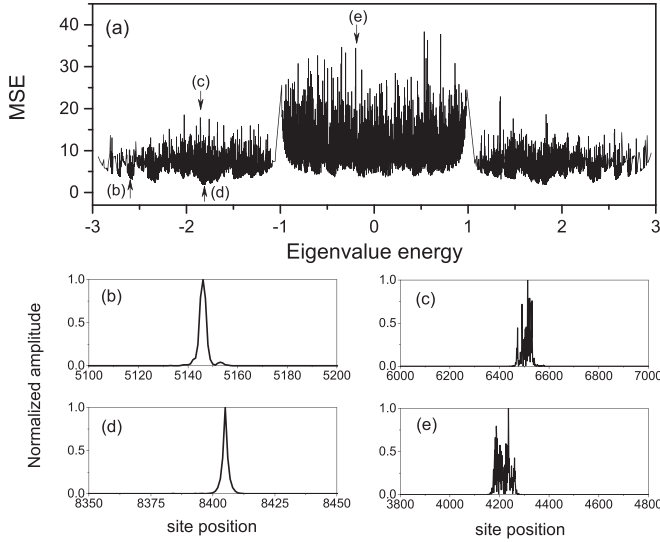
FIG. 4. (a) Mode spatial extent (MSE) of the Liouville structure. The arrows and corresponding letters label representative localized modes shown in (b)–(e) selected from the single-peak (b), (d) and multipeak (c), (e) populations.
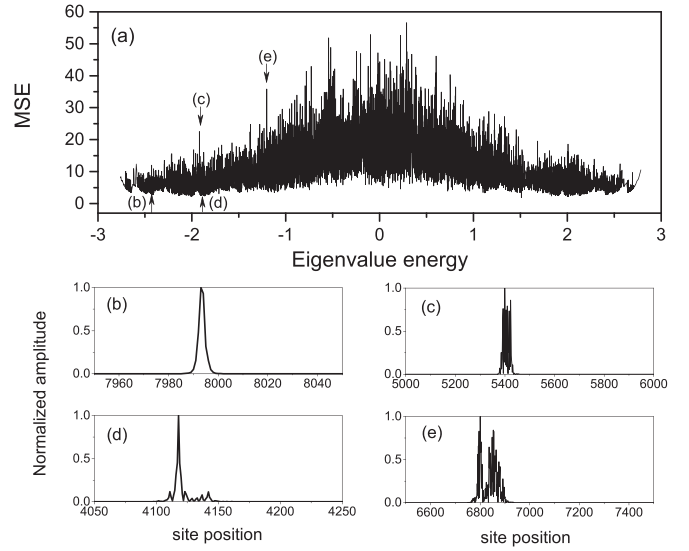

FIG. 5. (a) Mode spatial extent (MSE) of the Möbius structure. The arrows and corresponding letters label representative localized modes shown in (b)–(e) selected from the single-peak (b), (d) and multipeak (c), (e) populations.

designed to support only localized states in their spectra. In order to address this important question, we propose to exploit the intrinsic complexity of arithmetic functions and investigate the spatial localization properties of the Liouville and Möbius structures by computing the mode spatial extent (MSE) of all their eigenmodes. The corresponding results for the Legendre sequence of QRs are summarized in Appendix A. The MSE parameter quantifies the spatial extension of an eigenmode ψ_i of the system at the energy E_k and is defined as [35]

$$\mathrm{MSE}(E_k) = \frac{\left(\sum_{n=1}^{N} |\psi_n(E_k)|^2\right)^2}{\sum_{n=1}^{N} |\psi_n(E_k)|^4}, \tag{8}$$

where N is the total number of sites in the system. Therefore, the MSE estimates the number of sites in the structure over which the eigenmode intensity is mostly concentrated.

In Fig. 4(a) we show the computed MSE values across the entire energy spectrum of the Liouville structure. Since the system has 3×10^4 sites and the maximum MSE value is less than ≈ 40, all modes in the spectrum are strongly localized over a significantly smaller region compared to the total size of the system. This is confirmed by the spatial profiles of the representative eigenmodes displayed in Figs. 4(b)–4(e), which correspond to the spectral positions indicated by the arrows in Fig. 4(a). Moreover, we found that the spectrum contains two types of modes with remarkably different spatial behavior: (i) Modes with a single-peak behavior that are strongly localized over only a few sites, as the ones reported in Figs. 4(b) and 4(d), and (ii) less localized modes with multipeak fluctuations, as in Figs. 4(c) and 4(e). A very similar MSE structure and localization behavior was also found for the Legendre sequence reported in Appendix A. On the other hand, our results for the Möbius structure, shown in Fig. 5, provide a different MSE spectrum with a slightly larger maximum value ≈ 55. This is consistent with the more homogeneous character

of the Möbius multifractal spectrum characterized by a significantly narrower $f(\alpha)$, as shown in Fig. 3, compared to the Liouville case. However, we found that all the eigenmodes of the Möbius structure are also strongly localized with either single-peak or multipeak spatial profiles. In Fig. 6 we show the proportion of each type of mode in the spectrum for all the investigated structures. Our analysis was performed for systems with increasing number of sites in order to rule out spurious finite-size effects. The results show that the fraction of single-peak ($\approx 10\%$) and multipeak modes ($\approx 90\%$) remains constant across a large range of sizes for all the investigated structures.

We then address the statistical distribution of the logarithm of the MSE values. In Fig. 7 we show the results of our analysis that consider all the modes as well as the two identified types of modes separately. Interestingly, in both cases we could fit the data with an excellent quality using Gaussian functions (dotted lines). This indicates a log-normal distribution of the MSE values, similarly to the case of uncorrelated
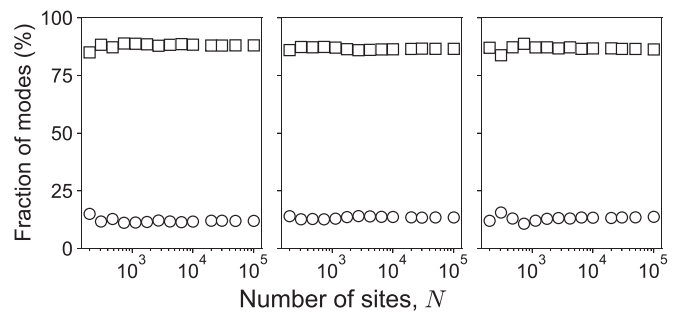

FIG. 6. Fraction of modes as a function of the number of sites N for the Möbius, Liouville, and Legendre sequence structures, respectively. Circles (squares) correspond to single-peak (multipeak) modes.
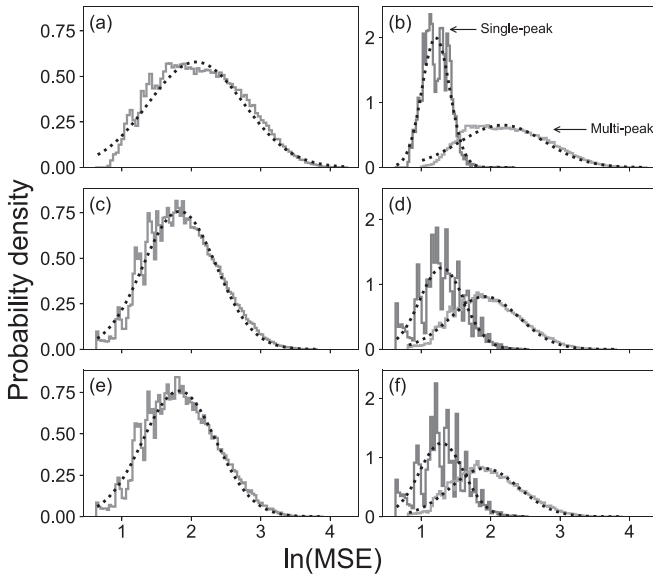
FIG. 7. Probability density of the logarithm of the MSE values of the eigenmodes for the (a), (b) Möbius, (c), (d) Liouville, and (e), (f) Legendre sequence structures. (a), (c), (e) Consider all the modes while (b), (d), (f) show the results for the two types of identified modes separately. The dotted lines are Gaussian fits. For this analysis we considered a large system with $N = 10^5$ sites.
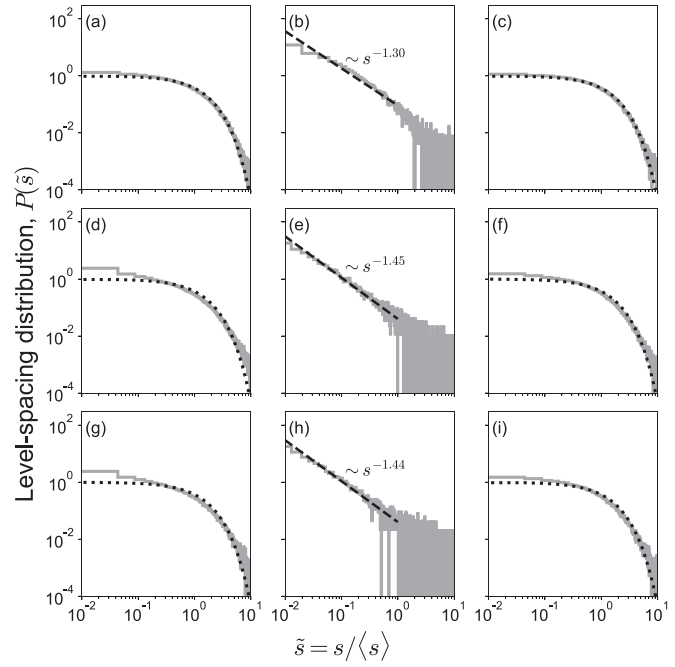

FIG. 8. Distribution of level spacing for the (a)–(c) Möbius, (d)–(f) Liouville, and (g)–(i) Legendre sequence structures. (a), (d), (g) Show the results obtained when considering all modes. (b), (e), (h) Show the results when analyzing single-peak modes only, whereas (c), (f), (i) when analyzing multipeak modes only. The dotted lines correspond to the Poisson distribution $P(\tilde{s}) = e^{-\tilde{s}}$. The dashed lines are best fits with the indicated models. For this analysis we considered a large system with $N = 10^5$ sites.

disordered systems in low dimensions [80]. This behavior reflects the uncorrelated nature of the "algorithmic disorder" that is intrinsic to the investigated arithmetic functions.

In order to better understand the nature of localization in the investigated systems we perform a statistical analysis of the level spacing that is often utilized to identify different transport regimes in closed (Hermitian) systems. In closed random systems, established results from random matrix theory (RMT) predict the suppression of level repulsion in the presence of localized states [81]. In these systems, spatially separate, exponentially localized modes hardly influence each other and can coexist at energies that are infinitely close. In particular, in the strong localization regime the level spacing statistics is described by the Poisson distribution [82]

$$P(\tilde{s}) = \exp(-\tilde{s}), \qquad (9)$$

where $\tilde{s}$ is the nearest-neighbor level spacing normalized to the average spacing. The results of our analysis are shown in Fig. 8 where we considered separately the level statistics of all the modes from the one of single-peak and multipeak mode types. In particular, we find an inverse exponential Poisson distribution in all the structures when all the modes are analyzed, as shown in Figs. 8(a), 8(d), and 8(g) for the Möbius, Liouville, and quadratic residue sequence, respectively. The same behavior also occurs when considering the level spacing statistics of the multipeak modes, shown in Figs. 8(c), 8(f), and 8(i). In contrast, we discover a power-law distribution for the level spacing of the strongly localized single-peak modes, displayed in Figs. 8(b), 8(e), and 8(h). In the context of RMT, it has been shown that a power-law level spacing distribution is characteristic of the critical modes of complex systems with multifractal spectra, leading to sub-diffusive dynamics [46,75,83]. However, to the best of our

knowledge, a critical regime with power-law level spacing distribution has not been reported in relation to strongly localized single-peak (i.e., smooth) eigenmodes, which appears to be a characteristic, unique feature of the investigated multifractal spectra [46,75]. Further studies beyond the scope of this paper are needed to establish the exact nature of these deeply localized, single-peak eigenmodes.

In addition, it is important to compare the unique localization behavior discovered in the investigated systems with the one that characterizes uncorrelated random systems within the well-known 1D Anderson model. In order to do this, we consider an ensemble of disordered structures in which V_n in Eq. (1) is taken as a random variable uniformly distributed: $[-W/2, W/2]$ with $W = 2$. As a relevant figure of merit, we have considered the scaling of the average MSE with respect to the size of the system, and we show our results in Fig. 9. Interestingly, we find that the average MSE obtained in the Anderson model is larger than the one of the introduced deterministic aperiodic systems across the entire range of sizes that we have analyzed. We also note the weak dependence of the MSE values on the system size, showing that the localized regime is already achieved in structures with relatively small sizes. Moreover, the lowest average MSE values are displayed by the Liouville and the quadratic residue sequence potentials, which feature the most inhomogeneous multifractal spectra [i.e., broader $f(\alpha)$ spectra] compared to the Möbius and the random systems. Therefore, our results demonstrate not only that all the modes are strongly localized in the
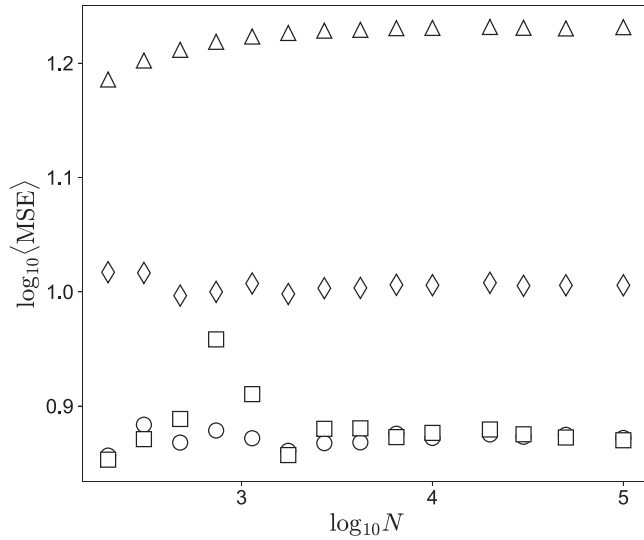
FIG. 9. Scaling analysis of the average MSE values as a function of the system's size for the Möbius (diamonds), Liouville (circles), and Legendre sequence (squares) structures as compared to the Anderson model (triangles). In the latter we perform an ensemble average over realizations of the random potential V_n uniformly distributed in $[-W/2, W/2]$, with $W = 2$. At least 10^6 eigenvalues are considered for each size of the random structure.

types of structures that we have introduced, but also that they achieve stronger spatial localization compared to a traditional random system within the Anderson model. These findings underline the importance of strong multifractal correlations in arithmetic function-based structures for the engineering of electronic and photonic structures with enhanced localization behavior across the entire energy spectrum.

V. CONCLUSIONS

In summary, we investigated the spectral and localization properties of deterministic aperiodic structures generated from the Liouville, Möbius, and Legendre functions that are primary examples of multiplicative arithmetic functions in number theory. We systematically studied their energy spectra using MDFA and demonstrated multifractal scaling properties associated to their unique structural complexity. We then investigated their eigenmodes and localization properties, demonstrating that all structures support localized modes with characteristic single-peak and multipeak distributions independently of the system's size. Moreover, we discovered a log-normal MSE distribution and two different regimes of level spacing statistics that demonstrate the absence of level repulsion, features that characterize strong localization in the investigated structures. Finally, we establish a stronger degree of mode localization in the investigated structures compared to the eigenmodes of the Anderson model. These results underline the relevance of the inherent multifractal complexity of arithmetic functions for the design and engineering of localized waves of particular importance to cold-atom experiments in aperiodic potentials and to optoelectronic structures with enhanced light-matter interactions without the involvement of disorder.
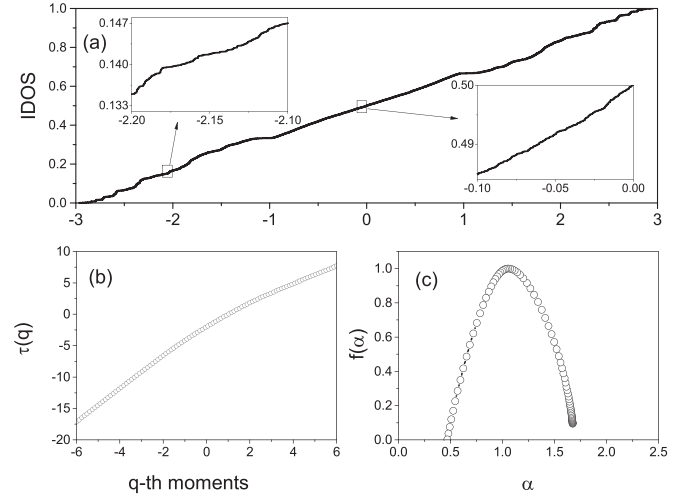

FIG. 10. (a) Integrated density of states (IDOS) for the structure based on the Legendre sequence for the distribution of quadratic residues. The insets show magnified views of the IDOS within the small rectangular regions of interest identified. (b) Mass exponent (scaling function) $\tau(q)$ and (c) multifractal spectrum $f(\alpha)$ of the spectrum shown in (a).

APPENDIX A: RESULTS FOR THE LEGENDRE SEQUENCE

In this Appendix we report the results on the binary Legendre sequence (the initial value $L_0 = 0$ is neglected). In Fig. 10(a) we show the computed spectrum of the IDOS as a function of energy. The two insets magnify the IDOS within the representative small spectral regions identified by the corresponding arrows. Similarly to the cases of the Liouville and Möbius structures, the IDOS spectrum is monotonically increasing and features multiscale fluctuations and narrow plateau regions. The multifractal nature of this spectral measure is unveiled by MDFA analysis that we used to compute the mass exponent behavior [Fig. 10(b)] and the multifractal spectrum [Fig. 10(c)]. The results in Figs. 10(b) and 10(c) indicate strong multifractality in the investigated Legendre system, with a width $\Delta f(\alpha)$ of the multifractal spectrum that is similar to the one of the Liouville structure, implying a comparable degree of nonuniformity.

In Fig. 11(a) we show the computed MSE values of the Legendre sequence across the entire energy spectrum. Since the system has maximum size $p = 29\,989$ sites, the results clearly demonstrate the strong spatial localization of all the eigenmodes in the spectrum with a maximum MSE ≈ 40. Representative spatial profiles for the two identified types of localized modes are shown in Figs. 11(b) and 11(d) for single-peak and 11(c) and 11(e) for multipeak eigenstates. Overall, we found that spectral and localization behavior of
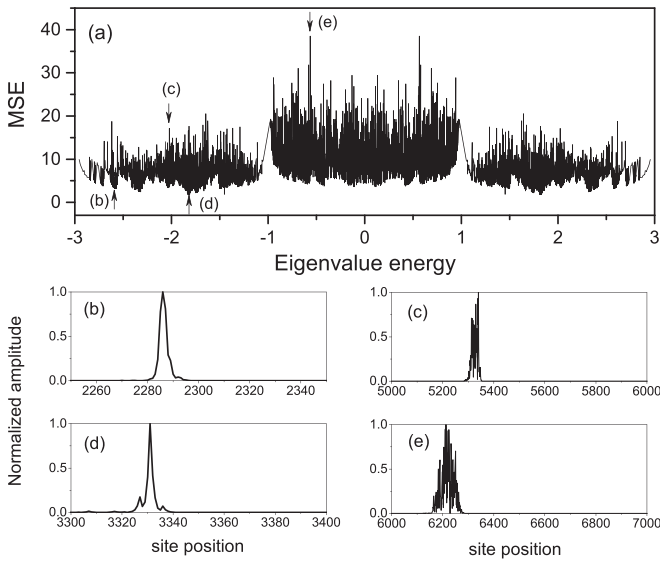
FIG. 11. (a) Mode spatial extent (MSE) of the Legendre sequence structure. The arrows and corresponding letters label representative localized modes shown in (b)–(e) selected from the single-peak (b), (d) and multipeak (c), (e) populations.

the Legendre function is qualitatively similar to the one of Liouville structures discussed in the main text.

APPENDIX B: STRUCTURAL CORRELATION PROPERTIES

In this Appendix we discuss the structural correlation properties of the investigated arithmetic sequences. The $\lambda(n)$ function manifests a complex aperiodic behavior with oscillations at all scales and appears to be an uncorrelated random function with no discernible patterns. Many fundamental results of number theory can be deduced assuming the uncorrelated randomness of $\lambda(n)$, most notably the PMT. In addition, the Liouville function provides an elementary reformulation of the RH that makes it equivalent to the statement that an integer number has equal probability of having an odd or an even number of prime factors [67,84]. This remarkable statement of the RH clearly demonstrates the fundamental role played by algorithmic "randomness" in number theory. Consistently, we found that the Liouville sequence has a flat autocorrelation (i.e., a peak at the origin and constant value otherwise), as shown in Fig. 12(a), which is similar to the
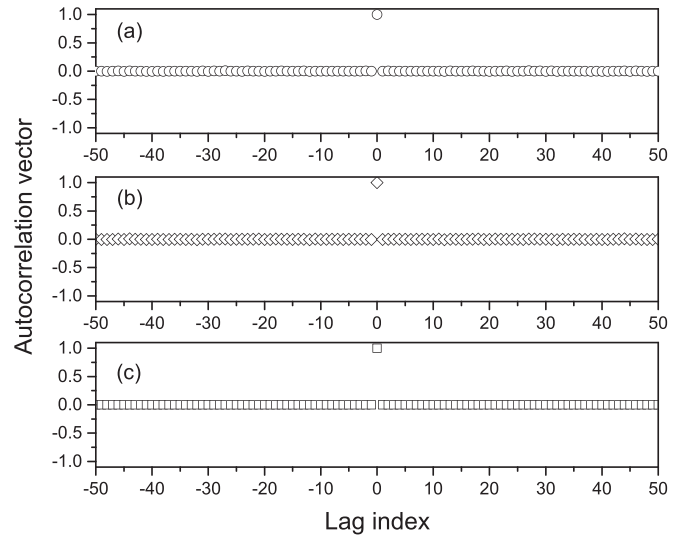

FIG. 12. Normalized autocorrelation vector of the (a) Liouville, (b) Möbius, and (c) Legendre sequences. Results for structures with $N = 10^5$ sites are shown here.

ideal two-valued autocorrelation function established for the Legendre sequence. The (periodic) autocorrelation of the sequence L_n is defined as

$$c_m = \sum_{n=0}^{p-1} L_n L_{n+m}, \qquad (B1)$$

where all the indices are considered mod p. The observed bilevel autocorrelation implies a flat power spectrum, similarly to the case of a Bernoulli random process. We found that this interesting correlation/spectral property is also exhibited by the Möbius sequence, as demonstrated in Fig. 12(b). While no analytical results exist in this case, the behavior is consistent with the fact that the mean value of the Möbius sequence is known to vanish [66]. Finally, in Fig. 12(c) we show the normalized autocorrelation of the Legendre sequence, which features an absolutely continuous correlation measure. This exhibits a theoretical two-valued autocorrelation property with amplitude values $c_m = p - 1$ for $m \equiv 0 \bmod p$ and $c_m = -1$ for $m \neq 0 \bmod p$. This characteristic behavior can be derived directly either by using the properties of the Legendre symbol or by expressing the Legendre sequence through the index associated to a primitive root (i.e. the discrete logarithm). The details of these classical derivations can be found in [72,73].

[1] P. Sheng, *Introduction to Wave Scattering, Localization and Mesoscopic Phenomena* (Springer, Berlin, 2006), Vol. 88.

[2] E. Akkermans and G. Montambaux, *Mesoscopic Physics of Electrons and Photons* (Cambridge University Press, Cambridge, 2007).

[3] L. Dal Negro, *Optics of Aperiodic Structures: Fundamentals and Device Applications* (Pan Stanford Publishing, Singapore, 2014).

[4] L. Dal Negro, *Waves in Complex Media* (Cambridge University Press, Cambridge, 2022).

[5] P. W. Anderson, Absence of diffusion in certain random lattices, Phys. Rev. **109**, 1492 (1958).

[6] D. Levine and P. J. Steinhardt, Quasicrystals: A New Class of Ordered Structures, Phys. Rev. Lett. **53**, 2477 (1984).

[7] E. Abrahams, *50 Years of Anderson Localization* (World Scientific, Singapore, 2010), Vol. 24.

[8] E. M. Barber, *Aperiodic Structures in Condensed Matter: Fundamentals and Applications* (CRC Press, Boca Raton, FL, 2008).

[9] F. M. Izrailev, A. A. Krokhin, and N. Makarov, Anomalous localization in low-dimensional systems with correlated disorder, Phys. Rep. **512**, 125 (2012).

[10] C. Janot, *Quasicrystals: A Primer* (Oxford University Press, Oxford, UK, 1994).

[11] L. Dal Negro and S. V. Boriskina, Deterministic aperiodic nanostructures for photonics and plasmonics applications, Laser Photon. Rev. **6**, 178 (2012).

[12] M. Kohmoto, B. Sutherland, and C. Tang, Critical wave functions and a Cantor-set spectrum of a one-dimensional quasicrystal model, Phys. Rev. B **35**, 1020 (1987).

[13] M. Quilichini, Phonon excitations in quasicrystals, Rev. Mod. Phys. **69**, 277 (1997).

[14] H. Q. Yuan, U. Grimm, P. Repetowicz, and M. Schreiber, Energy spectra, wave functions, and quantum diffusion for quasiperiodic systems, Phys. Rev. B **62**, 15569 (2000).

[15] A. Jagannathan, The Fibonacci quasicrystal: Case study of hidden dimensions and multifractality, Rev. Mod. Phys. **93**, 045001 (2021).

[16] R. Ketzmerick, G. Petschel, and T. Geisel, Slow Decay of Temporal Correlations in Quantum Systems with Cantor Spectra, Phys. Rev. Lett. **69**, 695 (1992).

[17] R. Ketzmerick, K. Kruse, S. Kraut, and T. Geisel, What Determines the Spreading of a Wave Packet?, Phys. Rev. Lett. **79**, 1959 (1997).

[18] S. Roche, G. Trambly de Laissardière, and D. Mayou, Electronic transport properties of quasicrystals, J. Math. Phys. **38**, 1794 (1997).

[19] L. Dal Negro and S. Inampudi, Fractional transport of photons in deterministic aperiodic structures, Sci. Rep. **7**, 2259 (2017).

[20] S. Thiem and M. Schreiber, Wavefunctions, quantum diffusion, and scaling exponents in golden-mean quasiperiodic tilings, J. Phys.: Condens. Matter **25**, 075503 (2013).

[21] M. A. Bandres, M. C. Rechtsman, and M. Segev, Topological Photonic Quasicrystals: Fractal Topological Spectrum and Protected Transport, Phys. Rev. X **6**, 011016 (2016).

[22] F. Baboux, E. Levy, A. Lemaître, C. Gómez, E. Galopin, L. Le Gratiet, I. Sagnes, A. Amo, J. Bloch, and E. Akkermans, Measuring topological invariants from generalized edge states in polaritonic quasicrystals, Phys. Rev. B **95**, 161114(R) (2017).

[23] W. Steurer and D. Sutter-Widmer, Photonic and phononic quasicrystals, J. Phys. D: Appl. Phys. **40**, R229 (2007).

[24] E. L. Albuquerque and M. G. Cottam, Theory of elementary excitations in quasiperiodic structures, Phys. Rep. **376**, 225 (2003).

[25] A. Poddubny and E. Ivchenko, Photonic quasicrystalline and aperiodic structures, Phys. E (Amsterdam) **42**, 1871 (2010).

[26] D. Barache and J. M. Luck, Electronic spectra of strongly modulated aperiodic structures, Phys. Rev. B **49**, 15004 (1994).

[27] E. Maciá, Exploiting aperiodic designs in nanophotonic devices, Rep. Prog. Phys. **75**, 036502 (2012).

[28] E. Maciá, The role of aperiodic order in science and technology, Rep. Prog. Phys. **69**, 397 (2006).

[29] K. Ishii, Localization of eigenstates and transport phenomena in the one-dimensional disordered system, Prog. Theor. Phys. Suppl. **53**, 77 (1973).

[30] D. J. Thouless, Electrons in disordered systems and the theory of localization, Phys. Rep. **13**, 93 (1974).

[31] M. Y. Azbel and P. Soven, Transmission resonances and the localization length in one-dimensional disordered systems, Phys. Rev. B **27**, 831 (1983).

[32] M. Y. Azbel, Eigenstates and properties of random systems in one dimension at zero temperature, Phys. Rev. B **28**, 4106 (1983).

[33] J. Pendry, Quasi-extended electron states in strongly disordered systems, J. Phys. C: Solid State Phys. **20**, 733 (1987).

[34] J. Bertolotti, S. Gottardo, D. S. Wiersma, M. Ghulinyan, and L. Pavesi, Optical Necklace States in Anderson Localized 1D Systems, Phys. Rev. Lett. **94**, 113903 (2005).

[35] F. Sgrignuoli, G. Mazzamuto, N. Caselli, F. Intonti, F. S. Cataliotti, M. Gurioli, and C. Toninelli, Necklace state hallmark in disordered 2D photonic systems, ACS Photonics **2**, 1636 (2015).

[36] D. H. Dunlap, H. L. Wu, and P. W. Phillips, Absence of Localization in a Random-Dimer Model, Phys. Rev. Lett. **65**, 88 (1990).

[37] S. N. Evangelou and A. Z. Wang, Localization in paired correlated random binary alloys, Phys. Rev. B **47**, 13126 (1993).

[38] H.-L. Wu and P. Phillips, Polyaniline is a Random-Dimer Model: A New Transport Mechanism for Conducting Polymers, Phys. Rev. Lett. **66**, 1366 (1991).

[39] J. Bellissard, Schrödinger operators with almost periodic potemntial: An overview, in *Mathematical Problems in Theoretical Physics*, Lecture Notes in Physics, Vol. 153 (Springer, Berlin, Heidelberg, 1982), pp. 356–363.

[40] J. Bellissard and B. Simon, Cantor spectrum for the almost mathieu equation, J. Funct. Anal. **48**, 408 (1982).

[41] J. Luck, Cantor spectra and scaling of gap widths in deterministic aperiodic systems, Phys. Rev. B **39**, 5834 (1989).

[42] J. Bellissard, Gap labelling theorems for Schrödinger operators, in *From Number Theory to Physics* (Springer, Berlin, 1992), pp. 538–630.

[43] J. Kaminker and I. Putnam, A proof of the gap labeling conjecture, Michigan Math. J. **51** (2003).

[44] E. Maciá, On the nature of electronic wave functions in one-dimensional self-similar and quasiperiodic systems, Int. Scholarly Res. Not. **2014**, 165943 (2014).

[45] T. Fujiwara, M. Kohmoto, and T. Tokihiro, Multifractal wave functions on a Fibonacci lattice, Phys. Rev. B **40**, 7413 (1989).

[46] I. Guarneri and G. Mantica, Multifractal Energy Spectra and Their Dynamical Implications, Phys. Rev. Lett. **73**, 3379 (1994).

[47] M. Tashima and S. Tasaki, Multifractal wave functions of a system with a monofractal energy spectrum, J. Phys. Soc. Jpn. **80**, 074004 (2011).

[48] S. Aubry and G. André, Analyticity breaking and anderson localization in incommensurate lattices, Ann. Isr. Phys. Soc. **3**, 133 (1980).

[49] G. Roati, C. DErrico, L. Fallani, M. Fattori, C. Fort, M. Zaccanti, G. Modugno, M. Modugno, and M. Inguscio, Anderson localization of a non-interacting Bose–Einstein condensate, Nature (London) **453**, 895 (2008).

[50] P. G. Harper, Single band motion of conduction electrons in a uniform magnetic field, Proc. Phys. Soc. London, Sect. A **68**, 874 (1955).

[51] M. Schreiber, S. S. Hodgman, P. Bordia, H. P. Lüschen, M. H. Fischer, R. Vosk, E. Altman, U. Schneider, and I. Bloch, Observation of many-body localization of interacting fermions in a quasirandom optical lattice, Science **349**, 842 (2015).

[52] T. Kohlert, S. Scherg, X. Li, H. P. Lüschen, S. Das Sarma, I. Bloch, and M. Aidelsburger, Observation of Many-Body Localization in a One-Dimensional System with a Single-Particle Mobility Edge, Phys. Rev. Lett. **122**, 170403 (2019).

[53] D. R. Grempel, R. E. Prange, and S. Fishman, Quantum dynamics of a nonintegrable system, Phys. Rev. A **29**, 1639 (1984).

[54] J. Chabé, G. Lemarié, B. Grémaud, D. Delande, P. Szriftgiser, and J. C. Garreau, Experimental Observation of the Anderson Metal-Insulator Transition with Atomic Matter Waves, Phys. Rev. Lett. **101**, 255702 (2008).

[55] L. Kroon, E. Lennholm, and R. Riklund, Localization-delocalization in aperiodic systems, Phys. Rev. B **66**, 094204 (2002).

[56] M. Queffélec, *Substitution Dynamical Systems–Spectral Analysis* (Springer, Berlin, 2010), Vol. 1294.

[57] F. Iglói, L. Turban, and H. Rieger, Anomalous diffusion in aperiodic environments, Phys. Rev. E **59**, 1465 (1999).

[58] L. Kroon and R. Riklund, Absence of localization in a model with correlation measure as a random lattice, Phys. Rev. B **69**, 094204 (2004).

[59] R. Wang, F. A. Pinheiro, and L. Dal Negro, Spectral statistics and scattering resonances of complex primes arrays, Phys. Rev. B **97**, 024202 (2018).

[60] F. Sgrignuoli, S. Gorsky, W. A. Britton, R. Zhang, F. Riboli, and L. Dal Negro, Multifractality of light in photonic arrays based on algebraic number theory, Commun. Phys. **3**, 106 (2020).

[61] L. Dal Negro, Y. Chen, S. Gorsky, and F. Sgrignuoli, Aperiodic bandgap structures for enhanced quantum two-photon sources, J. Opt. Soc. Am. B **38**, C94 (2021).

[62] L. Dal Negro, Y. Chen, and F. Sgrignuoli, Aperiodic photonics of elliptic curves, Crystals **9**, 482 (2019).

[63] L. Dal Negro, D. T. Henderson, and F. Sgrignuoli, Wave transport and localization in prime number landscapes, Front. Phys. 490 (2021).

[64] F. Sgrignuoli and L. Dal Negro, Subdiffusive light transport in three-dimensional subrandom arrays, Phys. Rev. B **101**, 214204 (2020).

[65] T. M. Apostol, *Introduction to Analytic Number Theory* (Springer, Berlin, 1998).

[66] W. Schwarz, J. Spilker, and J. Spilker, *Arithmetical Functions* (Cambridge University Press, Cambridge, 1994), Vol. 184.

[67] P. Borwein, S. Choi, B. Rooney, and A. Weirathmueller, *The Riemann Hypothesis: A Resource for the Afficionado and Virtuoso Alike* (Springer, New York, 2008).

[68] R. Sivaramakrishnan, *Classical Theory of Arithmetic Functions* (Routledge, New York, 2018).

[69] J. Goldman, *The Queen of Mathematics: A Historically Motivated Guide to Number Theory* (CRC Press, Boca Raton, FL, 1997).

[70] M. R. Schroeder, The unreasonable effectiveness of number theory in science and communication (1987 Rayleigh lecture), IEEE ASSP Mag. **5**, 5 (1988).

[71] M. Schroeder, Number theory, IEEE Potent. **8**, 14 (1989).

[72] M. Schroeder, *Number Theory in Science and Communication: With Applications in Cryptography, Physics, Digital Information, Computing, and Self-Similarity* (Springer, Berlin, 2009).

[73] B. K. Horn, Interesting eigenvectors of the Fourier transform, Trans. R. Soc. S. Afr. **65**, 100 (2010).

[74] E. E. Fenimore and T. M. Cannon, Coded aperture imaging with uniformly redundant arrays, Appl. Opt. **17**, 337 (1978).

[75] T. Geisel, R. Ketzmerick, and G. Petschel, New class of level statistics in quantum systems with unbounded diffusion, Phys. Rev. Lett. **66**, 1651 (1991).

[76] J. W. Kantelhardt, S. A. Zschiegner, E. Koscielny-Bunde, S. Havlin, A. Bunde, and H. E. Stanley, Multifractal detrended fluctuation analysis of nonstationary time series, Phys. A (Amsterdam) **316**, 87 (2002).

[77] E. A. Ihlen, Introduction to multifractal detrended fluctuation analysis in matlab, Front. Physiol. **3**, 141 (2012).

[78] C.-K. Peng, S. V. Buldyrev, S. Havlin, M. Simons, H. E. Stanley, and A. L. Goldberger, Mosaic organization of dna nucleotides, Phys. Rev. E **49**, 1685 (1994).

[79] K. Falconer, *Fractal Geometry: Mathematical Foundations and Applications, 3rd Edition* (Wiley, Chichester, UK, 2014).

[80] A. D. Mirlin, Statistics of energy levels and eigenfunctions in disordered systems, Phys. Rep. **326**, 259 (2000).

[81] M. L. Mehta, *Random Matrices* (Elsevier, Amsterdam, 2004).

[82] F. Haake, Quantum signatures of chaos, in *Quantum Coherence in Mesoscopic Systems* (Springer, New York, 1991), pp. 583–595.

[83] P. Cvitanovic, I. Percival, and A. Wirzba, *Quantum Chaos–Quantum Measurement* (Springer, New York, 2013), Vol. 358.

[84] H. Montgomery, A. Nikeghbali, and M. T. Rassias, *Exploring the Riemann Zeta Function* (Springer, Cham, 2017).